

THE ORIGINS OF CHEMOMECHANICAL EFFECTS IN THE LOW-LOAD INDENTATION HARDNESS AND TRIBOLOGY OF CERAMIC MATERIALS

Steve J Bull^{†*}, Noushin Moharrami[‡], Sarah V Hainsworth[‡], and Trevor F Page[†]

*[†]School of Chemical Engineering and Advanced Materials,
Newcastle University
Newcastle upon Tyne
NE1 7RU, UK.*

*[‡]Department of Engineering
University of Leicester
University Road
Leicester
LE1 7RH*

Abstract

We have used high-resolution techniques (nanoindentation, atomic force microscopy) to further isolate and identify environmental effects previously reported as possibly affecting both the microindentation response of a range of ceramic materials and their tribological behaviour. In order to make meaningful comparisons, these new experiments have been conducted alongside conventional Knoop and Vickers microhardness experiments conducted under identical conditions on the same samples. A range of polycrystalline, single crystal and amorphous ceramic materials have been studied including some only available as coatings. Our results show that thin adsorbate-modified layers (of dimensions $\sim 1\text{nm}$) are almost invariably present on all the materials studied but their presence is not directly identifiable by nanoindentation in most cases even if it does affect friction response. However, in crystalline materials, (1012 sapphire and ZnO), we have been able to distinguish a further softening effect seen as a thicker layer (tens of nm) and believed associated with an adsorption-induced near-surface band-structure change affecting the motion of charged dislocations. This produces a measurable softening that is clearly evident in nanoindentation tests but less clear in microindentation tests. Finally, we present conclusions on the suitability of indentation testing for studying these phenomena, together with the implications of chemomechanical effects for influencing tribological performance and, thus, materials selection.

Keywords

Chemomechanical effects, nanoindentation, microindentation, friction, chemisorption, band-structure

*Corresponding author; e-mail: steve.bull@ncl.ac.uk, tel: 0191 208 7913. Other authors; Noushin.moharrami@ncl.ac.uk; svh2@leicester.ac.uk; trevor.page@ncl.ac.uk

1.0 Introduction

The long-term environmental sensitivity of the surface mechanical properties of materials has long been recognised and properties such as creep, fracture and fatigue are known to be susceptible to changes in environment. A particular sub-group of these phenomena concerns the short-term effects of environment on the indentation hardness of ceramic materials, which, in the past, have sometimes been observed in small-scale near-surface-sensitive experiments such as microindentation tests. These effects are often collectively referred to as Rehbinder effects after the pioneering work of Rehbinder [1, 2] over 80 years ago. However, they are believed to be vitally important in controlling the tribological properties of ceramics and ceramic engineering coatings which show a marked dependence on the test environment [3, 4] and a number of mechanisms have been suggested to explain behaviour including chemisorption affecting near-surface mechanical properties.

Although there is a considerable body of literature on phenomenological environmental effects in ceramic tribology, there is less work on the environment-induced changes in specific near-surface mechanical properties of ceramics, particularly studies establishing clear controlling mechanisms [5-7]. Since there has also been considerable controversy over whether such effects were reliably observed in microhardness studies [8, 9], or whether they were errors of observation or other artefacts, previously proposed possible mechanisms will be reviewed briefly.

The work presented in this paper involves results from experiments using higher spatial resolution techniques than microindentation, such as instrumented indentation techniques (nanoindentation) and atomic force microscopy imaging, used to try and resolve some of the previous controversies and ambiguities emerging from microindentation studies, thus enabling clearer mechanisms to be established for chemomechanical effects. Our overall aim is to improve materials selection for tribological performance with due attention to in-service environmental effects.

1.1 Previous microindentation studies

Microhardness studies of possible chemomechanical effects appear to have been triggered by a phenomenon known as "anomalous indentation creep", whereby short-term static hardness was observed to progressively decrease with time (of the order of seconds) at rates far faster than any conventional creep process. These were observed by Westbrook and co-workers [10, 11] and Westwood and co-workers [12-14] in a number of ceramic systems. For instance, Hanneman and Westbrook [10] investigated the time dependence of the hardness of a range of materials measured in a range of solvents and reported even a short-term softening of about 10-20% in the presence of adsorbed water layers on various ceramic materials including zinc oxide and alumina. By contrast, metals were found to have a constant, time-independent hardness in all solvents. However for ionic, covalent and Van der Waals solids, different results were found. In dry toluene the hardness was time independent but, in moist air, a lower time-dependent hardness decrease was observed. Westbrook and Jorgensen [11] also found that different crystallographic orientations of the same material had different environmental sensitivities.

Generally, studies such as [12] appeared to confirm that the presence of adsorbates controlled such chemomechanical effects, but the observed phenomena effects were of variable reliability and magnitude. Later, in work involving microhardness tests on a range of ceramic

materials in alcohols of different chain lengths, Czernuszka and Page [15, 16] demonstrated that the precise nature of the adsorbed species could influence the observed effects.

Previous studies have usually involved microhardness testing as a convenient and tractable means of measuring suitable very-near-surface mechanical properties. However, the errors in measurement of small-scale indentations are comparable to the size of the changes measured after environmental exposure and, therefore, the existence of any chemomechanical effects and mechanisms have not been convincingly demonstrated or proven in many cases.

Despite this, a variety of mechanisms have been proposed to explain these observations as discussed in detail by Westwood et al. [13]:-

- (1) Adsorption creating differences in the way that changes in surface charges might interact electrostatically with charged near-surface structural defects (e.g. dislocations and vacancy clusters etc.). However, such effects have been shown to be several orders of magnitude too small to explain the observed hardness changes [13].
- (2) The motion of dislocations that produce surface slip steps could be affected by surface active environments changing the surface energy of the material [13]. If this were reduced then, thermodynamically, dislocation propagation might become easier. However non-surface-emergent dislocations (e.g those forming loops or terminating on internal boundaries) were also found to be affected by these surface active environments. Thus, this mechanism seems both small in magnitude and unlikely.
- (3) Changes to indenter/substrate friction caused by surface adsorbates acting as a lubricating ‘boundary layer’ which could modify frictional drag in the region where interfacial sliding is required as the indenter moves against, and through, the material being tested [13]. Bowden and Tabor [17] noted that the presence of adsorbate films on ceramic materials reduced the friction between the surface and a diamond slider. Similar effects could be happening for “quasi-static” indentations, but the amount of relative sliding during such an indentation test is small.
- (4) Dislocation interactions with adsorbates on, or slightly within, the surface. These fall into two categories, namely direct ‘conventional’ mechanical interactions such as dislocation drag or ‘solid solution hardening’, and possible further electronic interactions.
 - a. The first of these effects can be eliminated as it would generally be expected to result in a hardening of the surface layer, though some mechanisms such as dislocation egress (by dislocations either being attracted towards, or repelled from, the surface by image forces from any substantial soft surface layer [e.g.18]) might produce the required softening. However, such layers are believed to be too thin to create significant image force effects.
 - b. The second such effect (i.e. more intense electronic or charge interactions) mechanisms have neither been demonstrated nor proven. However, it has been suggested [13] that adsorption results in the bending of the electron energy bands near the crystal surface and this will affect the energy required for dislocation motion in ceramic crystals where dislocations often possess necessarily charged cores [18]). This is similar to the theory of Hirsch [19] for the effect of dopants on the mechanical properties of semiconductors where significant changes in dislocation mobility may be induced by only small

dopant levels.

- (5) In general, maximum hardness has been associated with minimising the surface charge (at least as measured by the electrochemical ζ -potential [20] which measures surface charge densities). At this condition, the mobility of dislocations in the surface layer (as measured by etch-pitting techniques) has been observed to be minimized. Thus, any change in surface charge (due to adsorbates) results in an increase in dislocation mobility and a reduction in hardness. As measured by changes in the characteristic etch-pit rosettes around indentations, the mobility of edge dislocations was affected to a greater extent than that of screw dislocations [13] but the mechanisms were unspecified.

Of relevance here – and for discussion later - is that, in our earlier work on ion-implantation treatments for ceramic surfaces, we found that low-dose Ti^+ ion implantation was found to reduce the observed chemomechanical effect in the microindentation response of single crystal MgO tested using a Knoop indenter [21]. This was subsequently related to a reduction in the amount of adsorbed water [22]. However, this was only observable because of the very large/strong, reliably-observed chemomechanical effect observed in this particular crystalline oxide material [12, 14]. We also showed that this situation was created by titanium ions segregating towards the near-surface region as Ti^{4+} , helping to neutralize any near-surface charges, and thus removing the (presumed) driving force for water to be adsorbed [22]. Such surfaces are still free of significant adsorbed water many years later. Such charge effects relate to (4b) and (5) above but, potentially, are a more powerful mechanism than (1).

1.2 Previous nanoindentation studies

Since the early 1990s there have been attempts to improve on microindentation methods to unambiguously demonstrate the existence of chemomechanical effects themselves while striving to provide a better basis for understanding their mechanisms [e.g.23-29].

Hainsworth and Page [23, 24] reported studies on 1012 single crystal sapphire wafers, cleaned, heated in air at 500°C to remove both physisorbed and chemisorbed water, quenched into various dry solvents, dried and indented in ambient laboratory air (RH ~50%) in a thermally-stabilised room. A Berkovich indenter (250nm tip end radius) was used and peak loads of <5mN chosen (producing maximum indenter displacements of <60nm). A markedly soft surface layer (<~5 nm thick) was observed in the load-displacement curves for virtually all samples and ascribed to a water-softened surface layer which affected the hardness measurements at very low penetration depths. Also, as witnessed by changes to both the loads needed to effect the elastic-plastic transition and the number of displacement ‘pop-ins’ associated with dislocation nucleation below the surface [30], it was postulated that a change in the stresses to trigger dislocation sources, or the stress to subsequently move dislocations away from their source, may also have been effected. Over a period of ~4 weeks, the behavior of samples quenched into various solvents, reverted to that displayed by water-exposed samples.

Gerberich et al [25-26] adopted a different approach using liquid drops to modify the surface chemistry during the indentation test. By this process they could follow the changes in surface mechanical properties as passive oxides are etched and reformed on metals. By contrast, Mann and Pethica [27] performed nanoindentation tests with the sample and indenter completely immersed in liquid. This approach led to the observation that the

hardness and contact modulus of GaAs could be increased by immersion in long-chain alcohols [28] and that the increase was dependent on the length of the chain [29]. Similar to the effects encouraged by constraining oils in hydrodynamic bearing systems, adsorbed organic molecules can support significant loads and sustain large elastic strains when confined between surfaces [31] and, similarly, will modify the load support in an indentation contact [32], and can result in observed frictional anisotropy in tribological applications [e.g 33].

Belde and Bull [34] showed that chemomechanical effects could be observed in multilayer optical coatings on glass but the extent of the effect was different for different coating materials. As well as surface effects from adsorbed water, it was shown that water penetration could also lead to changes at interfaces below the surface causing effects such as lubricating intercrystalline sliding during the deformation of coatings with columnar structures [24], or enhancing coating detachment around indentations [34].

2.0 Experimental

In the work reported here, nanoindentation tests have been performed on a range of bulk oxide and oxide coating materials to attempt to substantiate – or not – the validity of the chemomechanical effect mechanisms outlined in the previous sections.

2.1 Materials

A range of oxide ceramic materials were tested, including single crystal *1012* sapphire, polycrystalline zirconia toughened alumina, soda-lime silica glass and titanium, tin and zinc oxide coatings. The bulk materials were obtained from commercial suppliers and were allowed to interact with water in the environment by storage in a humid laboratory for several months before testing. The samples were placed in transparent plastic storage boxes in a dark cupboard when not being tested to reduce contamination from the storage media and the effects of light on the surface. Initial nanoindentation tests were performed on these as-received coatings before the samples were heated to greater than 100°C for 30 minutes with a hot air gun - to remove most of the weakly-bound physisorbed water, at least - before quenching into methanol from a newly opened sealed bottle. A short chain alcohol was chosen to minimize the load support from any organic adsorbate layer affecting the measured mechanical properties. The water content on the methanol was 0.05% after opening (Karl Fischer titration) and this did not change if the bottle was kept tightly sealed during use. After quenching into the solvent, to minimize water pick-up the samples were kept in sealed plastic containers; after testing the water content of the solvent in these containers was less than 1% according to hygrometry measurements. Nanoindentation tests were then carried out on these samples after removal from the solvent and drying with hot air in a humidity controlled laboratory (RH~50%). Finally the samples were immersed in distilled water for 24 hours and tested again.

Fully dense, adherent oxide coatings were deposited on soda-lime silica glass by magnetron sputtering at the Pilkington Technical Centre (Lathom, UK). The coating thickness was 400nm in all cases. The coatings spent at least 24hours in transit from the coater to the test laboratory in ambient air. Initial nanoindentation tests were performed on these coatings within a few days of their being produced. The samples were then left for several months before being tested again in storage boxes in a closed storage cupboard in a humid laboratory

as before. There was no measurable difference between these measurements and the samples after delivery indicating that most adsorbate-induced changes are complete within 24 hours of exposure. The samples were then heated to greater than 100°C for 30 minutes with the hot air gun before quenching into ethanol from a freshly opened sealed bottle. The water content of the ethanol was 0.1% after opening (Karl Fischer titration) and this did not change appreciably during the test programme here as the bottle was kept tightly sealed. After cooling (see later) nanoindentation tests were carried out on these samples after removal from the solvent and drying with hot air in the humidity controlled laboratory (RH~50%). Finally the samples were immersed in distilled water for 24 hours and tested again after drying.

In this study, coated samples were quenched in methanol and bulk material were quenched in ethanol due to availability of sufficient quantities of low water-content solvent. Tests on the bulk sapphire samples showed that there was no difference in hardness behavior when quenched into the two solvents.

2.2 Indentation testing

In order to make meaningful comparisons between the nanoindentation results and the microhardness observations of the past, nanoindentation experiments were conducted alongside conventional Knoop and Vickers microhardness experiments upon the same materials surfaces, in the same states and under identical conditions.

Microhardness testing was performed with a Shimadzu microhardness tester fitted with a new Vickers or Knoop indenter to minimize the effects of tip blunting which occurs when testing hard ceramic materials. Except when a direct comparison with nanoindentation data was undertaken, all microhardness tests used the Knoop indenter due to its higher surface specificity and the possibility of more accurate indentation diagonal measurements at low penetration depth. However, all such tips have some degree of ‘chisel shape’ and even new ones are only sharp to a typical radius of ~400nm (at best) which essentially limits the contact depths at which plastic deformation can be induced by contact-induced, sub-surface shear stresses and thus ‘plasticity-softened’ or ‘plasticity-hardened’ surface effects sought. The effect of tip sharpness on the generation and position of contact-induced, near-surface, shear stresses is discussed by Page and Bull [35]. Prior to testing the tips were cleaned by sonication in isopropyl alcohol. The Vickers tip used had a 1µm wide chisel edge. The tip radius was measured from SEM images as 420nm across the chisel edge and greater than 1µm along its length,

All indentations were performed under standard laboratory conditions (ambient temperature, humidity 40-80% laboratory air (this is important for reliable data acquisition– see section 3.1), with a 15s dwell time, and ‘dead’ loads ranging from 150mN to 5N (see the results sections for the depth penetrations at these loads in each material). Hardness was calculated from the average of twenty indentation diagonals which were measured with the standard optical system of the microhardness tester. Measurements of indentation diagonals are limited to ±500nm by this method due to the resolution of the standard reflected light microscope which can lead to a ~25% error at the lowest test loads used here so the indents were remeasured by scanning electron microscopy to improve accuracy in these cases. The diagonals were carefully aligned with the *2201* reference edge on the single crystal *1012* (pseudo-cubic R-plane) sapphire samples chosen to minimize any effects of crystalline anisotropy.

Nanoindentation testing was carried out with two generations of continuously recording indentation testers. Initial experiments were carried out with a Nanoindenter 2 fitted with a new Berkovich tip (end radius about 250nm determined from a fit of the Hertzian elastic contact equations for a sphere to the initial elastic part of the loading curve for indentations in fused silica) at peak loads between 1mN and 500mN both located in an environmentally controlled laboratory. Prior to testing the samples were left to thermally equilibrate in the test lab for four hours whilst the tips were cleaned in isopropyl alcohol and machine frame compliance and tip end-shape was calibrated according to the method of Oliver and Pharr [36]; this tip calibration was carried out using only indentations in fused silica where the contact depth was less than 200nm. Arrays of 50 indentations were performed with 50 μ m spacing between each and 10 indentations at each peak load. The loading and unloading rate was 200 μ N/s. An approach speed of 10nm/s was used and a change in contact stiffness of $\times 4$ was used to detect first contact with the surface. At this point the load and indenter displacement are zeroed and the indentation cycle is commenced; the typical cycle involves loading to peak load, unloading to 30% of the peak load, holding for 25s whilst monitoring displacement (for thermal drift correction) and then complete unloading. Hardness and contact modulus was calculated from the load-displacement curves produced after correcting for thermal drift by the method of Oliver and Pharr [36]. Only indentations where the load-displacement curve clearly showed that plasticity had occurred were used in the analysis.

Thus, 'depth' in our nanoindentation results refers to the depth of plastic deformation using standard relationships from the load-displacement data [36], while the microindentation 'plastic' depth results are measured from the lateral size of the residual plastic impressions allowing for standard geometrical relationships between the length and depth of the residual indentations (e.g 7:1 for Vickers, 30.5:1 for Knoop). Thus, both of these measurements should be independent of elastic surface flexure – but see section 3.2.

Lower load tests were performed using a Hysitron Triboindenter fitted with a sharp indenter tip (end radius 105nm from elastic contacts in fused silica) which had been calibrated as above. Prior to testing tips were cleaned in isopropyl alcohol and ten test indentations were made on fused silica and aluminium samples to check for tip wear and contamination effects – if these were found the tip was cleaned and recalibrated. Arrays of 100 indentations with 10 μ m spacing were performed at peak load from 100 μ N to 10mN in open loop control. In this case the approach speed was also 10nm/s and contact was detected by a measurable increase in load in the transducer head (greater than 1.8 μ N). At this point the load and displacement were zeroed and the indentation cycle commenced. Initially there is a hold period in which the machine drift (both piezo creep and thermal) is minimized and this is followed by a 40s hold at the minimum contact load to monitor thermal drift. A linear fit to the last 10s of this is used for thermal drift correction. After this the indenter is loaded at 100 μ N/s to the peak load where it is held for 4s to allow any creep stabilisation.

Since the Hysitron indentation head is mounted on a piezoelectric scanner, Atomic force Microscopy (AFM) scans of some of the impressions were carried out using the tip that made them. This allowed any evidence for the extrusion of softer material from between the indenter and sample to be sought together with any possible pile-up of softer material under or around the indentations. No evidence for either of these was observed. Again the machine compliance and tip shape were calibrated and the load-displacement curves analysed by the method of Oliver and Pharr [36] to determine hardness and contact modulus. The data from at least five indents was averaged at each load.

Low load indentation data is presented as both plots of hardness or contact modulus versus plastic-deformation depth (e.g. Figures 4 & 5) or as indentation load versus depth (**p- δ** plots) as in Figure 9. The p- δ plots are better at revealing the presence of soft surface layers in many cases since the experimental errors are only half the error in the calculated hardness.

2.3 Materials analysis and characterisation

All microhardness indentations and the 100 and 500mN indentations made by the Nanoindenter 2 were analysed by scanning electron microscopy to look for changes in indentation shape and topography and check the accuracy of the indentation diagonal measurements. We also examined whether any evidence existed for the extrusion of thin softened surface layers which have been seen with high resolution SEM around nanoindentations in silicon and germanium and arising from a very thin, softened, amorphised material under the indenter [37-38]. Smaller indentations from lower load tests were subjected to in-situ AFM analysis to seek the same information.

X-ray diffraction was used to confirm the identity of the materials and search for any significant volumes of water-induced reaction products. This showed that the oxide coatings on glass were X-ray amorphous (except for ZnO) and the composition and thickness of the coatings was confirmed using X-ray Photoelectron Spectroscopy (XPS) depth profiles and ellipsometry. A more detailed analysis of the surface structure was carried out using Raman spectroscopy to look for the presence of adsorbed-water-produced reaction-products. A summary of our structural findings is shown in Table 1.

Material	Sample form	Crystalline or amorphous	Surface reaction layer
Sapphire	Bulk single crystal	Crystalline	None
Zirconia toughened alumina	Bulk polycrystalline	Crystalline	None
ZnO	400nm coating on glass	Crystalline	None
SnO ₂	400nm coating on glass	Amorphous	None
TiO ₂	400nm coating on glass	Amorphous	None
Soda-lime glass	Bulk material	Amorphous	None but Leached surface after dishwashing
Fused silica	Bulk material	Amorphous	None
Titanium	Bulk alloy	Crystalline	Titanium oxide

Table 1: Structural details for the samples used in the investigation

3.0 Results and Discussion

3.1 The Effect of Relative Humidity on data reproducibility

Given the previous, controversial nature of the evidence for the existence of chemomechanical effect in microhardness data (where sought-for changes in behavior are usually of the order of the experimental errors), it is important to choose test conditions in which the measurements are sufficiently controlled to produce reliable data. Since it has previously been observed that the ambient humidity can have an influence on the hardness and tribological performance of alumina [e.g. 17, 39], some initial tests were undertaken to establish the extent to which humidity needs to be controlled to ensure reproducibility in the microhardness tests. This involved placing the microhardness tester in a humidity-controlled glove box and performing an array of 5mN Knoop indentations in sapphire at different ambient relative humidities from 0 to 100% according to the cabinet controller. Ten indentations were performed at each humidity value and the long indentation diagonal was measured for all indentations with the optical system of the microhardness tester after all indentations were complete and the glove box door could be opened. The system was left to equilibrate for one hour after each new humidity level was established. The results of these tests are shown in Figure 1. The error bars plotted in this figure are the standard error of the results from the measurements at each relative humidity (i.e. the error in the mean). Paired T-tests show that all hardness values are statistically lower than that for 0%RH, indicates that a water-related chemomechanical effect is present in sapphire. From these statistical tests it is also clear that there is a statistically significant difference in hardness between 0 and 30% RH and between 80 and 100% RH when compared to the rest of the data, there is a plateau of “stable” hardness between 40 and 80% RH where there is no statistically significant difference between the average measurements. Measurements made between these values of humidity should not be affected by the water in the ambient air and this humidity range falls within the standard control range of the laboratory where the nanoindentation testers are located. For this reason it is not expected that the ambient humidity in the test lab will affect the nanoindentation data.

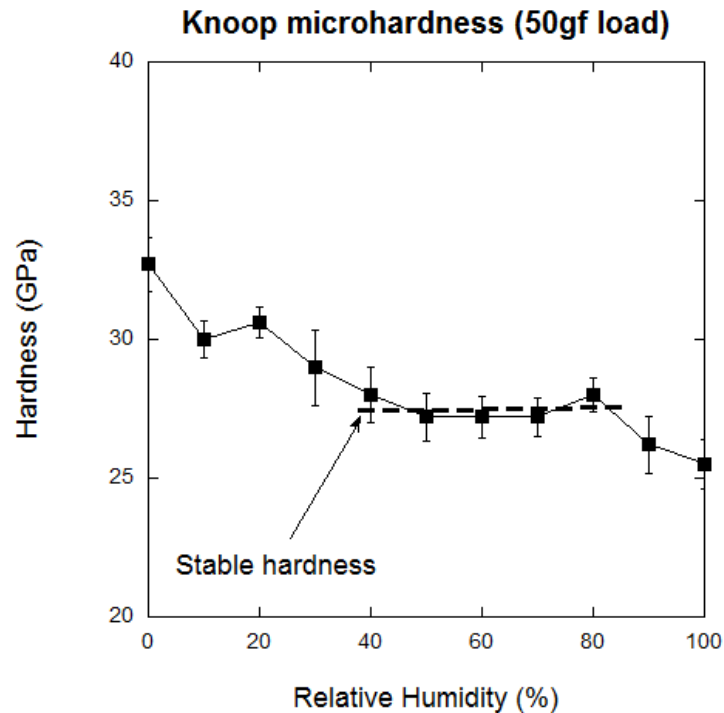


Figure 1: Variation of Knoop hardness with relative humidity for a sapphire substrate assessed by microhardness testing in a humidity-controlled glove box. The error bars represent the standard error for each datapoint. That all hardness values are statistically lower than that for 0%RH, indicates that a water-related chemomechanical effect is present in sapphire. However, there is a plateau of “stable” hardness, unaffected by changes in RH, between 40 and 80% RH (i.e. where the difference between the average measurements is not statistically significant as compared to the differences for the other datapoints).

Another source of variability comes from the manner in which the test is conducted. Some workers perform tests in air on samples which have previously been heated and then quenched into different liquids [22-24], essentially testing in a dry environment after liquid exposure. Other workers have placed a droplet of liquid on the test surface and indent through it [25-26] whilst yet others conduct the test with the sample and indenter completely immersed in the test liquid [27], essentially testing in a liquid environment. Both these latter approaches create potential problems because of the additional force effects, comparable with the indentation loads used in nanoindentation tests etc., arising either from buoyancy upthrust or meniscal drag from the liquids involved.

To investigate if this affects the measured results, microhardness tests were carried out on the same sapphire sample tested after exposure to distilled water and toluene using the solvent quenching and dry testing approach and the fully immersed testing methodology. After solvent quenching the sample was kept in the liquid for at least 24 hours before being removed and dried at 50°C with a hot air blower immediately before testing. For the immersion method, the sample was placed in an empty, shallow, flat-bottomed tray on the microhardness tester stage and the microscope focused on it. The indenter tip was then introduced above the sample and the tray filled with the test liquid so that both sample and indenter were immersed and left for 24h prior to testing. An array of ten indents was made at each of six different loads (10-300gf corresponding to penetration depths of <1000nm) in both experiments and the hardness determined from averaging measurements of the indentation diagonals made with the optical system of the microhardness tester.

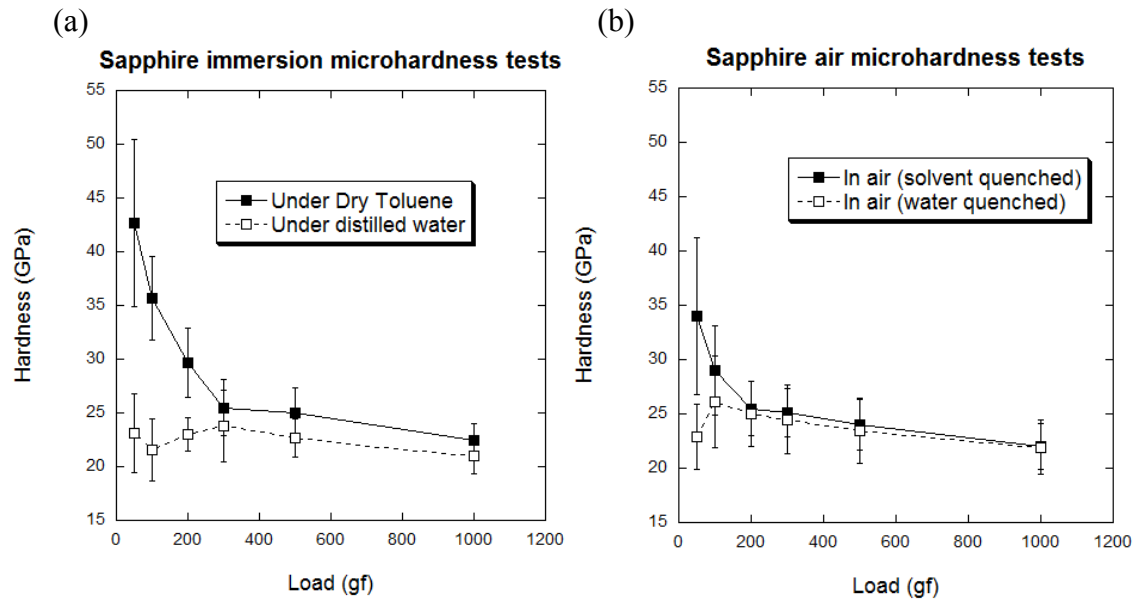


Figure 2: Variation of Knoop microhardness with load for sapphire tested after exposure to toluene and water (a) immersion testing and (b) solvent quench and dry testing. The difference in behavior – with an apparently larger chemomechanical effect seen across the whole load range when immersed in liquid – may be caused by buoyancy and meniscal effects reducing contact forces.

Figure 2 shows the results of these tests. It is evident that a very strong chemomechanical effect - i.e. the lowering of hardness - is observed at low test loads in the immersion tests (Figure 2a). However, this effect is less clear but still significant in the dry tests (Figure 2b), especially at loads of <200gf which corresponds to a penetration depth of ~2000nm. One further issue with the immersion test results is that the hardness values after water exposure lie below those in toluene across the whole load range whereas this is only the case for the low load tests in the dry testing. As mentioned previously, this is probably due to uncontrollable surface tension and buoyancy forces changing the effective test load in the immersion tests even after considerable cleaning of the indenter test shank [27]. The tests in dry air after environmental exposure appear more reliable and have been adopted in the rest of this study. However, even here, the magnitude of any chemomechanical effects appears reduced and microindentation testing – with hardness error bars of the order of any effect and only 1-2 standard loads available to make indentations in the critical range - is not really suitable for such studies.

There will still be a contribution to the indentation behavior from capillary forces even if the sample is tested in air as humidity may be drawn into the narrow gap around the indenter/sample contact. This effect increases as the gap closes (i.e. the radius of the tip increases in the low load tests here). Using the JKR approach [40] we can estimate the magnitude of the capillary force to be ~500 μ N and its effect on microindentation data is therefore minimal. For the sharper nanoindentation tips the magnitude of the effect is reduced but even for the lowest loads where plastic deformation is observed the effect on hardness is expected to be less than 5% which is much smaller than the differences observed when testing samples exposed to different environments.

3.2 To what extent are observed chemomechanical effects an artifact of the test method?

To aid comparison with previous microindentation results, Figure 3 compares hardness results from both Vickers microindentation and nanoindentation measurements made on a *1012* sapphire sample after heating and solvent quenching separately in methanol and distilled water and leaving for 24 hours. Indentation testing was performed immediately after drying the samples at 50°C.

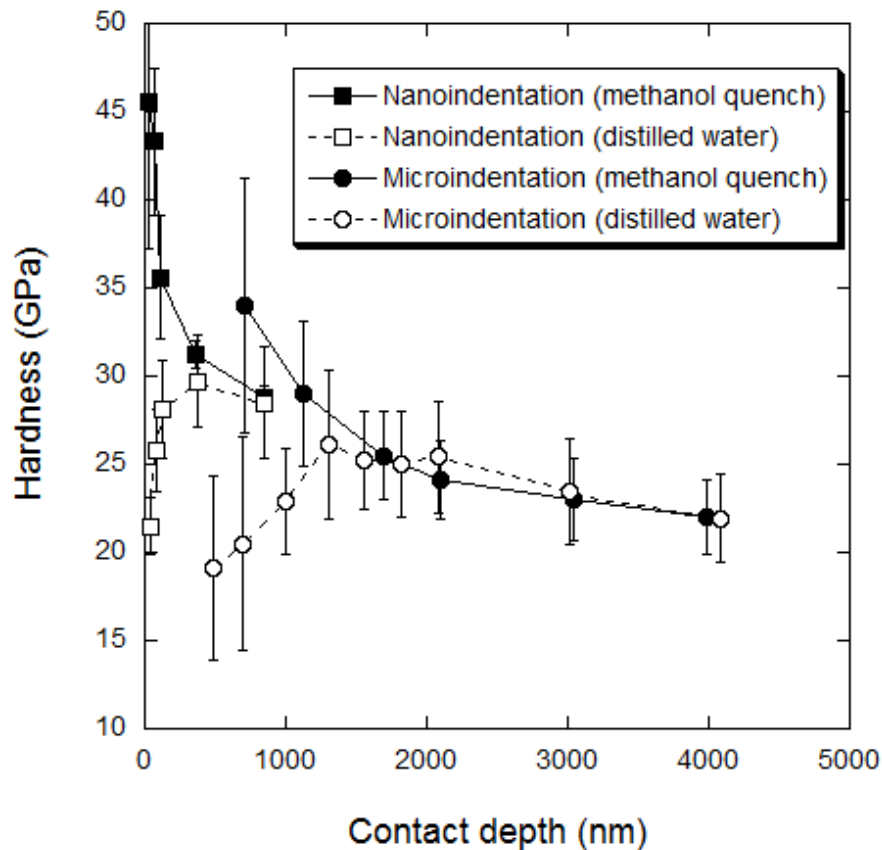


Figure 3: Comparison of the hardness of sapphire measured by different techniques after quenching in methanol and after 24h exposure to distilled water. While there appears to be a significant softening effect in the Vickers microhardness results, the nanoindentation results only show a significant reduction in hardness below contact depths of < 500nm.

For both micro- and nanoindentation tests, the hardness measured after methanol exposure increases as the contact depth is reduced. We believe that this is the normal “indentation size effect” usually observed when testing across different length scales in ceramics [e.g. 41, 42]. The microindentation data shows reasonable agreement with the nanoindentation data after methanol exposure but shows a greater rise at the lower end of its load range – even where this overlaps with the nanoindentation data – probably due to errors from measurement by light microscopy in the microindentation data and differing tip sharpness of the indenters used.

After water exposure, the near-surface hardness for both micro- and nanoindentation tests is reduced but the onset of this reduction occurs at greater contact depths for the microindentation data (~1500 nm) than in nanoindentation (<500nm). Again the larger-depth hardness data are consistent between the two techniques. This reduction in surface hardness is consistent with the effects of a soft surface layer [42]. However, given that the sample was treated in exactly the same way for the micro- and nanoindentation tests, it is likely that the apparently larger effect in the microindentation test is an artefact of the way that the measurements were performed, rather than the occurrence of a substantially-thicker water-affected layer in these cases only.

None of our indentation results are corrected for the small elastic recoveries known to occur in the indentation depth [43]. However, while any elastic surface flexure should not affect the results (this is accounted for in the nanoindentation case, and measurements made on the unloaded unflexed surface in microindentation), any significantly softened surface layer caught under the very ends of the Vickers indenter diagonals and supported by an underlying substrate which is still elastic, can locally deform plastically and thus make the indentation appear slightly longer than would be expected from substrate-controlled behaviour alone. The effect would be amplified by any pile-up of the softened material. This would have the effect of making the indentations look longer than expected and the surface appear commensurately (very slightly) softer. This effect would be more significant for the Knoop indenter, due to its smaller depth to long diagonal ratio, and it is more likely to reveal chemomechanical softened layers. However, it suffers from the same tip sharpness issues as the Vickers indenter. Thus nanoindentation testing was adopted in the rest of this study.

3.3 The behavior of sapphire

At the lowest indentation depths, there is a statistically-significant, difference between the nanoindentation hardness response of sapphire after exposure to methanol and water and this provides evidence for a water-mediated chemomechanical effect in the material. That the effect is related to the water in the environment can be seen in the low load range (and thus low contact depth) plots of Figure 4 which shows data from samples which have been tested as-received, after solvent quenching in methanol and then retested after solvent-quenching in water. Compared to the as-received samples, methanol exposure reduces the chemomechanical effect whereas further exposure to water increases it. In all cases, the samples which have been exposed to environmental water show a lower hardness than the rest in the near surface (upmost 40nm) region. That there is no significant difference in elastic contact modulus in these cases (as might be expected since none of the models in section 1.1 predicts an effect on elastic modulus), suggests that the modulus changes reported by Mann and co-workers [27-28] could have been an artefact of force reduction in their liquid immersion environments. In the present results, observed changes in contact modulus have been attributed to slight changes in tip calibration as they equally apply to samples tested in all environments.

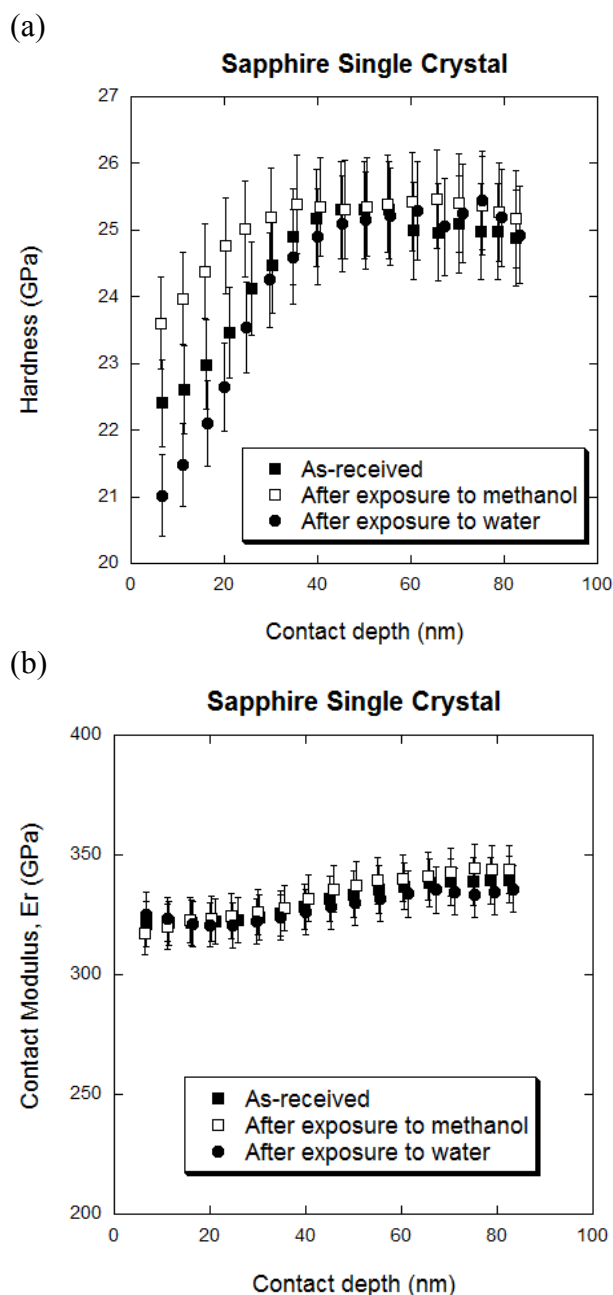


Figure 4: Changes in the chemomechanical effect in sapphire from the as-received state due to solvent quenching and subsequent exposure of the solvent-quenched sample to distilled water (a) hardness and (b) contact modulus. Water exposure does not affect the elastic response appreciably but does significantly affect the plastic response at contact depths less than 40nm. The slight reduction in contact modulus at the lower contact depths is due to small errors in the tip end-shape calibration since similar behavior is observed for all environments.

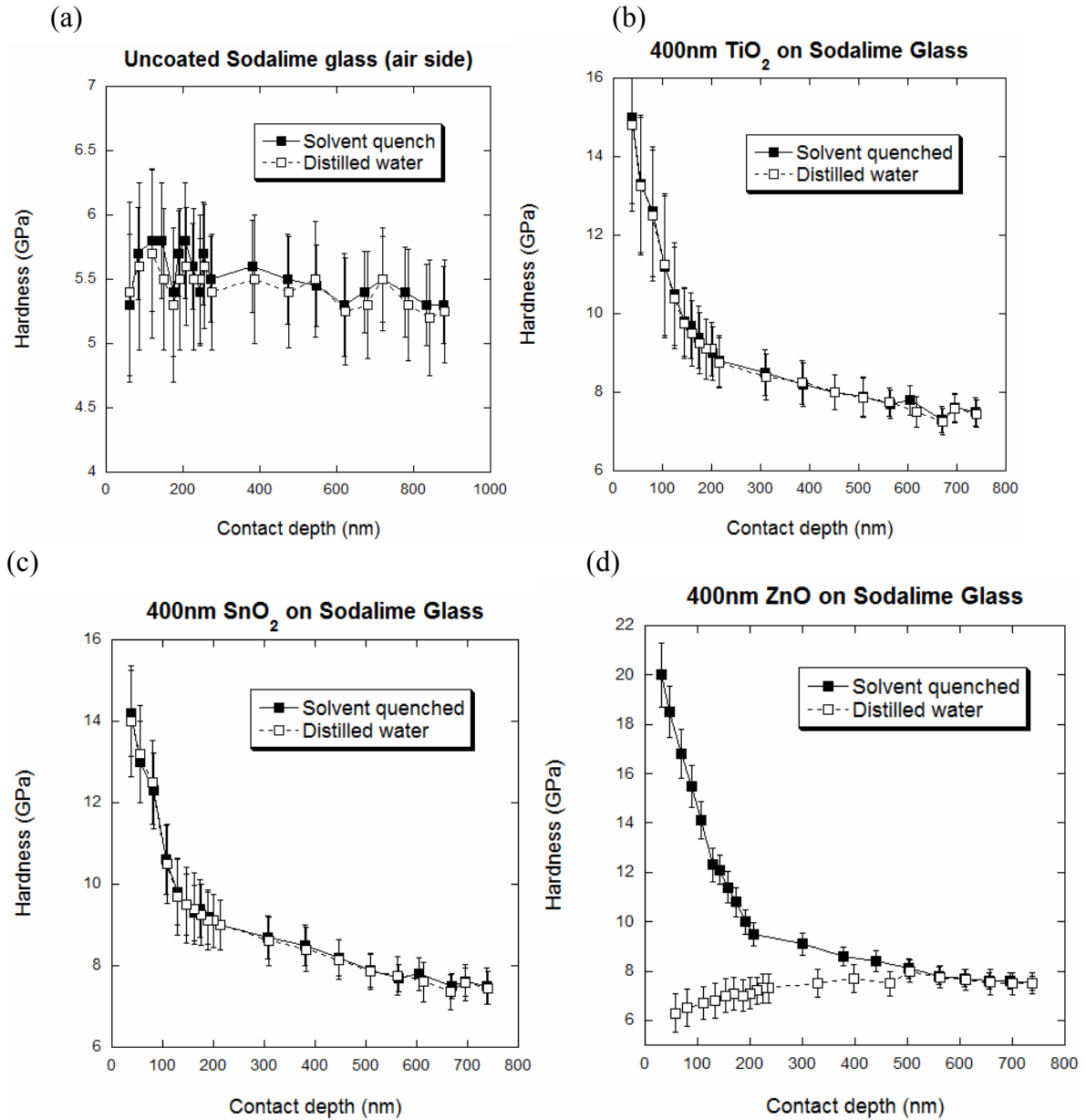


Figure 5: Variation of nanoindentation hardness with load for oxide coatings on a glass substrate as a function of environmental exposure, i.e. quenching in ethanol or immersion in distilled water (a) glass substrate, (b) TiO_2 , (c) SnO_2 and (d) ZnO . Only ZnO shows a significant chemomechanical effect that is a pronounced softening at contact depths, as large as 500nm. The low-load rises in hardness observed in all the other samples is due to these samples being in the form of coatings on a softer glass substrate, with the thin-film hardness dominating at shallow indentation depths.

3.4 How big is the chemomechanical effect for different materials?

A range of different oxide coatings on glass have been tested in air after solvent quenching in ethanol and distilled water and leaving for more than 24 hours. The nanoindentation hardness response of the glass substrate and three different oxide coatings is shown in Figure 5. The pronounced hardness increase at low contact depths for all the coated samples is due to the fact that the coating is harder than the substrate and what is measured is a composite hardness of coating and substrate once the contact depth exceeds 50 nm [44]. There may also be an indentation size effect in the ZnO case due to its crystallinity but this effect is minimal in the other amorphous coatings [45]. There is no apparent statistically significant chemomechanical effect for the soda-lime silica glass substrate, nor the titania and tin oxide coatings but a strong and significant chemomechanical is shown for ZnO.

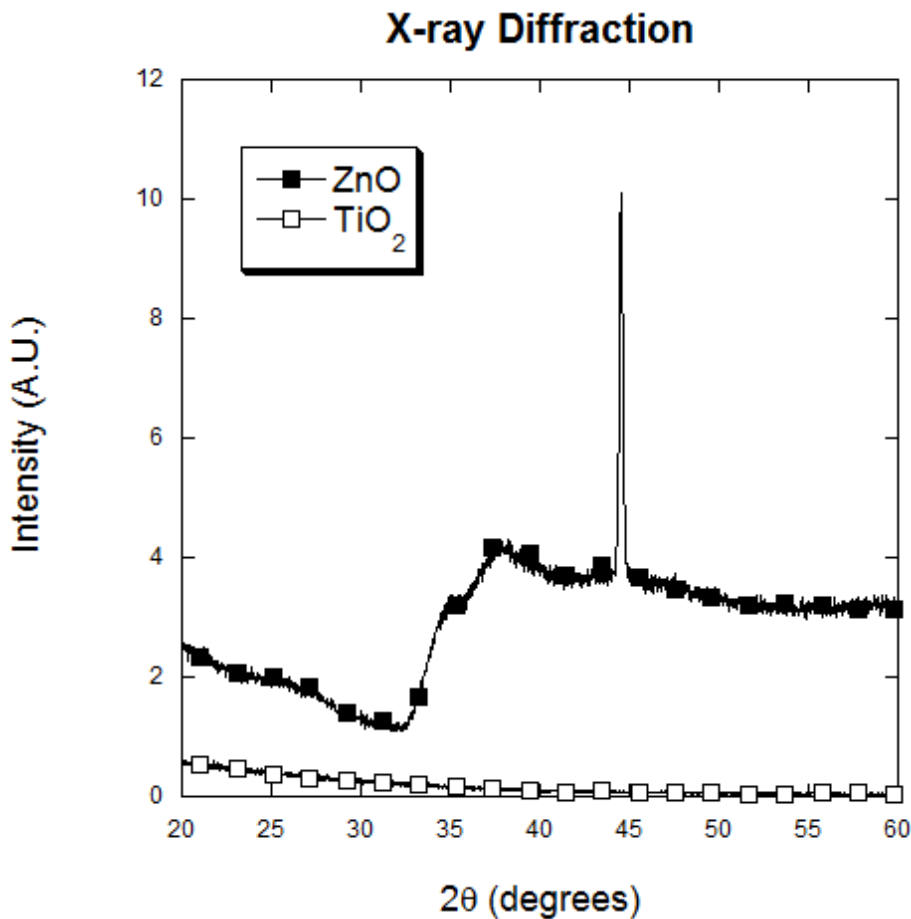


Figure 6: Comparison of XRD traces for 200nm TiO₂ and ZnO coatings on soda-lime glass. The TiO₂ is typical of the amorphous coatings seen in this study whilst the ZnO shows significant crystallinity as displayed by the sharp peak for ZnO.

The main difference between these coatings is that the ZnO coating has a high degree of crystallinity, whereas the other coatings are completely amorphous in X-ray diffraction experiments (Figure 6 and Table 1) though consisting of several amorphous ‘domains’ each having grown from an original coating nucleus during deposition. From section 1.1, of the possible mechanisms likely to be controlling chemomechanical effects, the only chemomechanical mechanism able to create an effect over tens of nanometers such as that observed in crystalline ZnO and sapphire is the *band-structure/charged dislocation-based model* [13]. *Thus we suggest that this is most likely to be controlling the larger-depth effects (5-500nm) seen in these cases.*

To explore the effects of this larger depth of chemomechanical-induced plasticity in ZnO further, Figure 7 shows AFM images, with profile sections through their centres, of low-load indentations in ZnO. In (a), no pile up or other evidence for the upthrust of material plastically displaced from the indentation is evident; while in (b) significant pile-up can be seen. This is characteristic of plastic flow occurring readily over a depth commensurate with the indentation depth and adds confirming evidence to the hypothesis of a chemomechanical effect influencing the plasticity properties of a surface layer thicker than a simple adsorption layer.

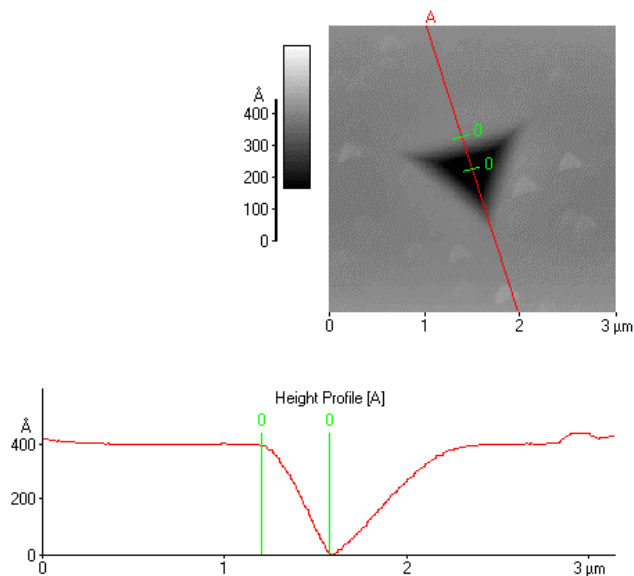
3.5 The p - δ response of samples with a thicker chemomechanically-softened layer

Figure 8(a) shows the nanoindentation load- displacement (p - δ) response for glass, both ethanol-quenched and water exposed. There is no apparent soft layer at the outset of the p - δ curve and the curves for both treatments are virtually superposable. However, in Figures 8(b) (sapphire) and 8(c) (ZnO), the presence of a soft surface layer is clearly visible in the early stage of the nanoindentation p - δ loading curve and the transition to harder behavior can be used as an estimate of the thickness of the chemomechanically-affected layer. For sapphire a soft layer ~5nm thick is present for the water-quenched sample (Figure 8(b)) which is not present for the solvent-quenched material. Also, at higher loads, the two curves shown in Fig 8(b) are not superposable simply by lateral shift; this suggests that the differences between these sapphire samples are still being detected at displacements larger than 5nm. Further, the water-affected curve displays no displacement pop-ins on loading, suggesting that dislocation nucleation no longer appears in sudden bursts but by some more gradual process. This is very similar to the previous observations of Hainsworth and Page [23].

A similar effect is seen for ZnO (Figure 8c), but here the thickness of the soft layer is much greater (~30nm), and the two curves are quite different to one another. Unlike the load-displacement curves shown in Figure 8b which look partly similar, here, this thicker soft layer dominates the load-displacement curve on the right of the figure and changes its whole appearance up to depths of ~150nm. Since the volume of softened material displaced by the indenter is smaller no similar effect was detected in sapphire.

Significantly, only the crystalline materials of Figs 8 (b & c) show recognizable chemomechanical effects in their low-load hardness response and only these same crystalline materials show recognizable differences in their p - δ responses – but the detailed depth over which they can be observed is materials’ dependent!

(a)



(b)

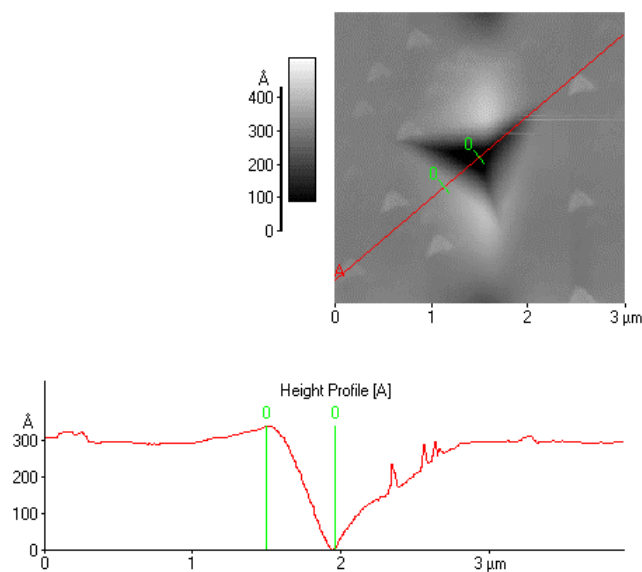


Figure 7: Atomic force micrographs of 6mN indents in ZnO coated sodalime glass (a) after quenching in dry ethanol and (b) after 24hours in distilled water. There is a difference in pile-up geometry between the two cases with considerable pile-up after water exposure, best detected in section where the scan line crosses the long edge of the impression. This surface-oriented flow of materials displaced from within the indentation indicates that water exposure significantly increases the plasticity of the sub-surface region of this sample. By contrast, all other samples exposed to water appeared as in (a) with no increase in pile-up.

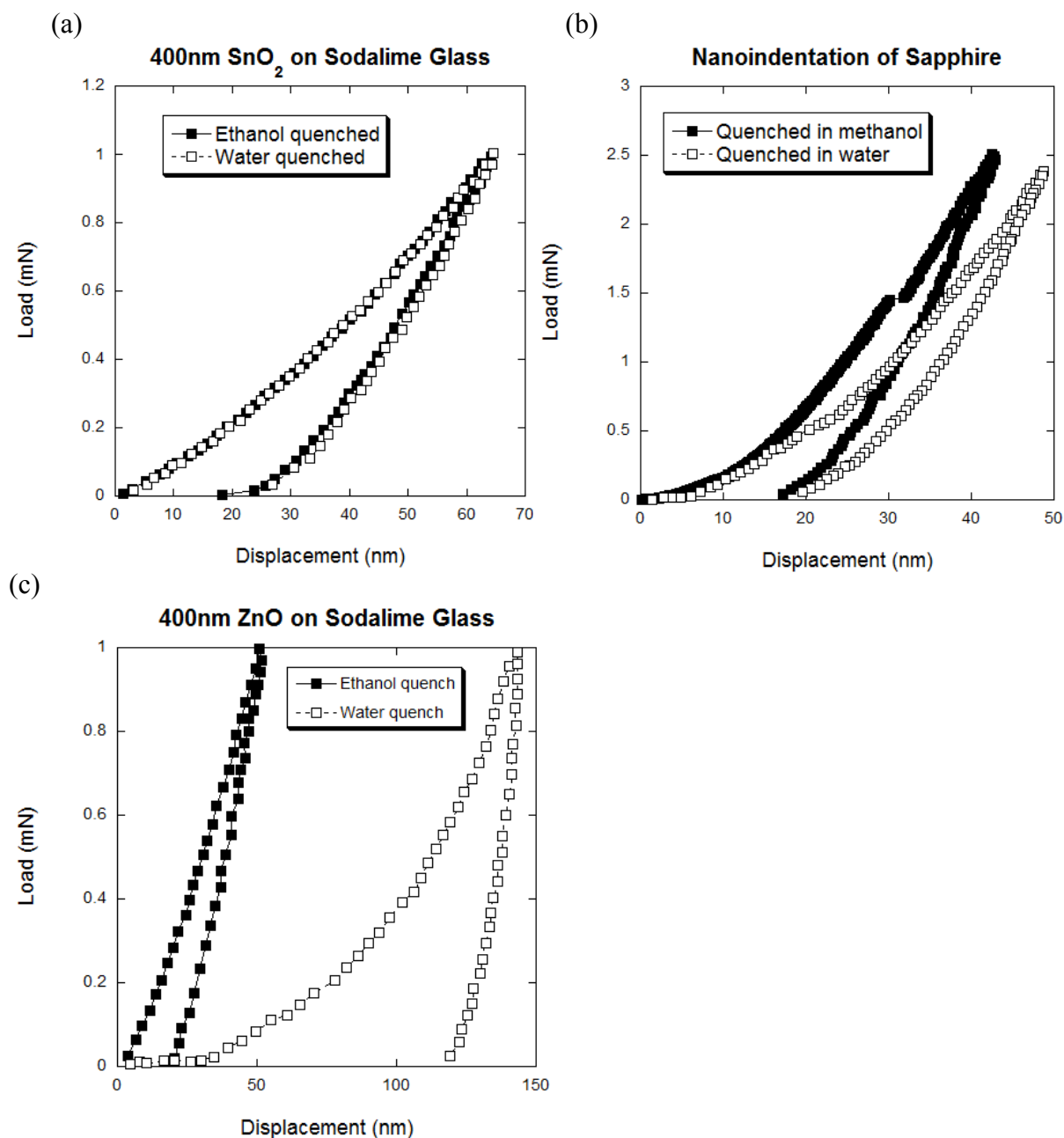


Figure 8: Comparison of nanoindentation load-displacement curved for samples tested after quenching in a non-polar solvent and after quenching in water (a) 400nm SnO₂ on sodalime glass, (b) single crystal sapphire and (c) 400nm ZnO on sodalime glass. See text for detailed comments.

3.6 Do adsorbate-induced phases control these ‘thicker’ layers of chemomechanical effects?

In order to identify any substantial adsorbate-formed phases controlling chemomechanical effects of the type observed here in sapphire [e.g. 46], Raman spectroscopy was used to identify any near-surface phases formed and the results shown in Fig 10. *We found no*

evidence of any near-surface hydroxides on the water-affected samples (strong Raman peaks at $305\text{-}325\text{cm}^{-1}$ and $535\text{-}580\text{cm}^{-1}$ are expected for the main aluminium hydroxide polymorphs [47] which are absent in Figure 9) or organic phases in the methanol-quenched samples.

Thus there is no Raman or X-ray diffraction evidence for gross reaction layers producing soft material after heating and solvent-quenching into water, nor any SEM or AFM evidence for extrusion of such softened layers from under the indenter during loading.

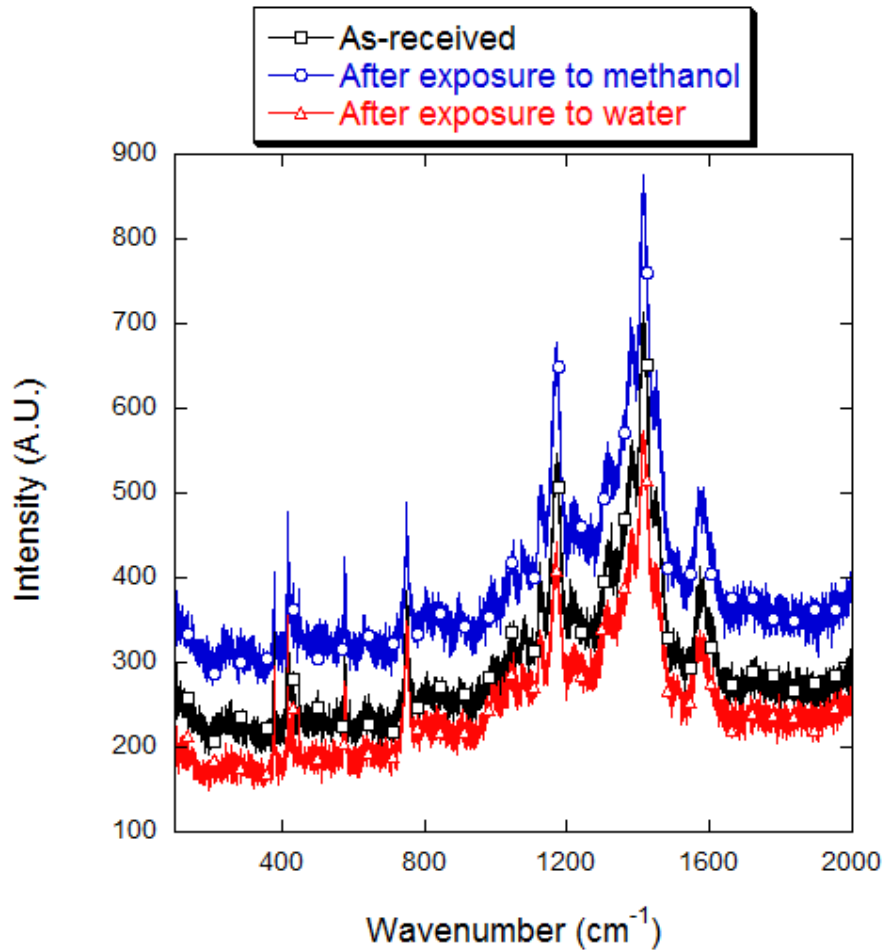


Figure 9: Raman spectra of sapphire surface before and after water and methanol exposure. There is no significant difference in all environments and no evidence of new phase formation after water exposure.

Following discussions of chemomechanical effect mechanisms in section 1.1 and the evidence we have presented so far, we postulate that there are two effects operating on the surfaces we have studied, namely

1. *A very thin adsorption-modified surface layer, possibly controlling friction by acting as a boundary lubricant but not apparent in low load indentation tests. We call this layer the adsorption-modified-layer (AML) and expect it to be $\leq 1\text{nm}$ thick.*
2. *A thicker region below any AML, occurring in crystalline oxide materials only, in which enhanced crystal plasticity can be induced by near-surface, adsorbate-controlled, band-structure bending. This seems to persist over scales of the orders of*

~10-50nm. We call this the band-modified-layer (BML). In here, the bending of the energy levels of the crystal near the surface will interact with the energy levels in dislocation cores with the observed effect of making plastic deformation easier.

3.6 Law of mixtures composite hardness calculations

Exploring hardness modelling of composite layered systems was triggered by our observations that we could not detect any softened surface layers in non-crystalline materials by low-load indentation techniques, even though other materials of this type reportedly have friction controlled by adsorbates.

There is also a previous observation of ours of our being able to scratch a softened (presumed) surface layer on fused silica with contact AFM where, again, we have no indentation evidence of a softened layer.

Modelling has been refined over several years from the pioneering work of Buckle [48] and addresses the hardness observed as an indenter penetrates a composite surface consisting of a coating on top of a substrate which may be harder or softer. In the case of a fused silica sample with a thin adsorbate modified layer (AML), the modelling confirms that the effect of the soft layer on hardness would not be observable under normal indentation testing conditions as it occurs at indentation depths where behaviour is predominantly elastic. For sapphire, a similar AML may be just about visible in very low load nanoindentation data if low-scatter experimental data is produced with a new sharp tip. However, the combined effect of this AML and the thicker band modified layer (BML) in sapphire has a much more significant effect on the hardness once elastic-plastic indentations are produced and this should be clearly visible in the measured nanoindentation hardness data.

This is also the case for the thicker BML on ZnO.

The Appendix has details of these calculations which support the conclusions at the end of the previous sections, but now demonstrate *why* AMLs alone – and even thin combined AML and BML – cannot be detected by current low-load indentation methods.

3.7 Adsorbates and friction

While AMLs cannot be detected by low-load indentation and since ceramic tribology seems to depend on them for friction control, we thought that it would be interesting to calculate their likely friction effects.

It is well known that the environmental contamination of coated glass can reduce the adhesion friction coefficient in a scratch test. For instance the friction coefficient against a PMMA slider of the TiO₂ coatings investigated in this study falls from greater than 0.5 immediately after cleaning to 0.32 after 24h exposure to laboratory air [45]. Similar results are obtained in scratch tests using a conospherical diamond indenter (5µm sphere radius) at 1mN normal load (Table 2). *Under these conditions no visible scratch track is produced and there is no plastic ploughing but the adhesion component of friction is reduced as the surface becomes more contaminated.*

Material	Coefficient of friction after cleaning by sonication in isopropyl alcohol	Coefficient of friction after 24 hours after re-exposure to laboratory air
TiO ₂	0.56	0.35
ZnO	0.52	0.32
SnO ₂	0.61	0.38

Table 2: Coefficient of friction of 400nm oxide coatings on glass tested with a conospherical diamond indenter at 1mN normal load and 1µm/s sliding speed.

All materials show a similar reduction in friction on contamination with surface adsorbates but only ZnO shows a strong chemomechanical effect implying that the indenter/substrate friction is not the cause of chemomechanical softening in the indentation test. Rather, at least part of the reduction in friction may be due to the formation of an AML. According to the simple analysis by Hutchings [49] the coefficient of friction, μ , for two planar materials sliding against each other, and deforming plastically, may be given by

$$\mu = \frac{12\tau_0\tau_i}{2\tau_i^2 + 11\tau_0^2} \quad (1)$$

where τ_0 is the bulk shear strength of the softer material and τ_i is the surface shear strength. The measured friction therefore depends critically on the ratio of surface shear strength to bulk shear strength and hence surface hardness to bulk hardness.

For sapphire tested at 50g load in sliding, the coefficient of friction varies from 0.25 after solvent quenching in toluene to 0.15 after solvent quenching in water when tested after drying. Using equation (1), it can be shown that the ratio of the surface shear strength of water exposed material to the surface shear strength of toluene exposed material is 0.64. Interestingly the ratio of surface to bulk hardness at 50g load in the data for the material exposed in the same manner is 0.67. *The consistency of these figures implies that it may be the changes in near-surface shear stresses which are controlling friction in these cases.*

The indenters used in hardness testing are all more akin to a flat punch than a sharp cone so any frictional contribution to the indentation deformation is expected to be small. It is also clear from finite element simulations of the development of an indentation that any sliding at the interface between the indenter and the coating is minimal and largely occurs at the edge of the contact [50]. *Thus, friction seems unlikely to be controlling any aspect of the indentation response of chemomechanically-affected materials, even crystalline ones.*

3.8 Chemomechanical effects on complex contacts

Contacts in real tribological systems show a very complex interplay between the contacting surfaces and the environment and it can occasionally be necessary to invoke chemomechanical effects to explain unlikely observed in-service behavior. One such case in in orthopedic implants; in a recent study it was observed that zirconia toughened alumina (ZTA) femoral heads showed scratch damage in the taper joint with a titanium alloy stem. The surface hardness of the titanium is only about 6-8GPa and considerably lower than the 17GPa hardness of the ZTA and is not expected to be able to scratch it. However, once implanted in the human body the both components are exposed to aqueous conditions at a temperature of 37°C. In such conditions the titanium alloy will oxidise forming a surface

oxide [51] with a hardness of about 15GPa (Figure 10b) whilst the ZTA undergoes chemomechanical softening and its hardness is reduced to a similar level (Figure 10a). The titanium oxide produced is x-ray amorphous and shows no chemomechanical softening. Given the now similar average hardness of the two contacting surfaces it is possible that harder asperities in the oxidized titanium may cause abrasive damage in the alumina, *thus altering the expected rank order of wear based on bulk hardness values alone*.

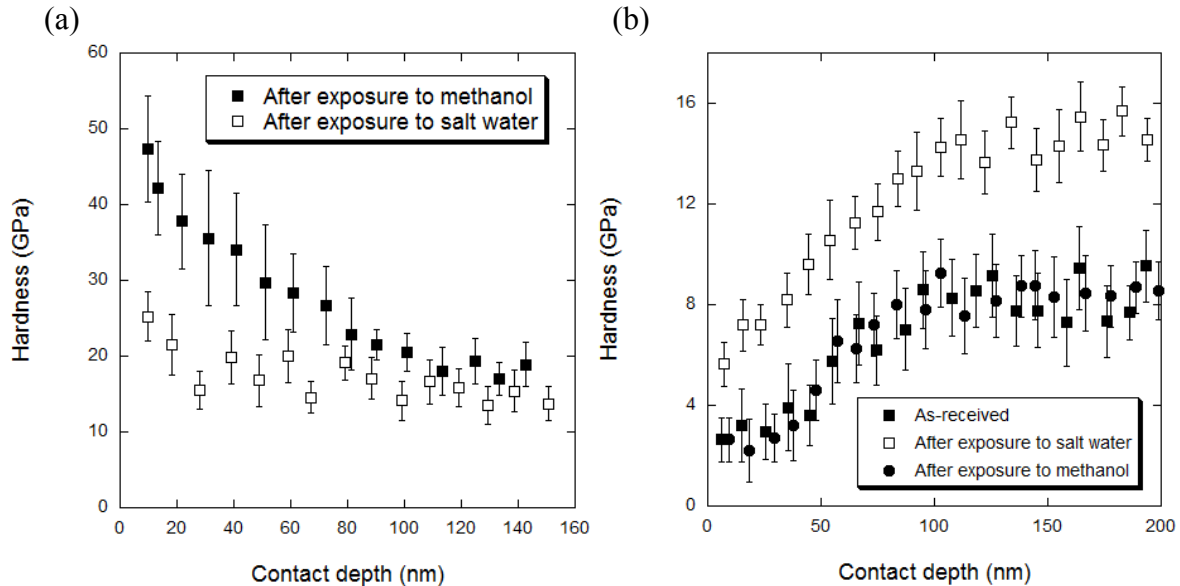


Figure 10: Hardness as a function of indenter displacement for (a) zirconia toughened alumina (ZTA) and (b) titanium alloy after different environmental exposure. The titanium alloy oxidises in water but the oxide is amorphous and does not show chemomechanical effects. The crystalline ZTA shows chemomechanical softening.

Similar observations have been made of the wear of alumina fibre guides by the titania whitener in synthetic fibres in the textiles industry [52] and in other soft-on-hard wear systems [53].

4 CONCLUSIONS

- Chemomechanical effects exist and influence the near-surface mechanical responses of ceramic oxide materials.
- The effects are caused by adsorption of water (and possibly other species) but are limited to shallow near-surface depths – typically <1nm thick for simple adsorbed layers or 10s of nm for more complex effects.
- We have shown the presence of at least two effects –
 - Thin water-softened layers (<1nm thick and materials-dependent) which can modify friction responses but are too thin to influence the indentation response of materials. *We call this layer the adsorption-modified-layer (AML).*
 - A thicker region below any AML, occurring in crystalline materials only, in which enhanced crystal plasticity can be induced by near-surface, adsorbate-controlled, band-structure changes/bending. This seems to persist over scales

of the orders of $\sim 5\text{-}30\text{nm}$. *We call this the band-modified-layer (BML)*. In here, the bending of the energy levels of the crystal near the surface will interact with the energy levels in dislocation cores with the observed effect of making plastic deformation easier.

- In practice the AML and BML are probably not present as discrete layers but will merge into each other.
- The total combined thickness of the AML and BML determines whether a material may be described as having a “strong” chemomechanical effect (e.g. the effects in MgO, ZnO and sapphire). Thus the linkages between materials strength, band structure, bandgap defect states and surface charge-induced band bending promise fertile areas of future research.
- A simple volume law-of-mixtures hardness model may explain some of the uncertainties and controversies apparent in the past microindentation-dominated literature. Not only has modeling shown how thin softened layers can affect hardness responses at contact depths greater than the thickness of the layer itself, but it has also clarified minimum limits for the detection of these layers by low-load indentation dependent upon tip sharpness and experimental errors.
- Because of this, low-load (depth-sensing) indentation experiments offer superior ways for investigating the presence of some of these thicker layers than conventional microhardness testing.
- The changes to depth ‘pop-ins’ in nanoindentation suggests that, in crystalline materials, further effects in the BML could involve either dislocation nucleation processes or the stress required for the subsequent glide of dislocations away from their sources.
- Chemomechanical effects detectable by low-load indentations may not reflect the changes in friction caused by these – or even thinner undetectable layers – in ceramic-based tribosystems. Here the changes in near-surface shear strengths are important rather than hardness per se. For fused silica, our AFM images confirm this important lubricating role even when no properties for scratchable layers can be determined by low-load indentations – i.e. the layer is otherwise ‘invisible’.
- However, softened surface layers of reduced hardness over some depth can alter the rank hardnesses of tribo-components thus altering relative abrasive wear rates of the oxides thought of as otherwise protecting metallic systems.
- Whether such effects occur in crystalline, non-oxide ceramics without a surface oxide layer is, as yet, unexplored and may offer a fruitful area for future studies.

5 Acknowledgements

The authors would like to thank Krishna Belde for providing some of the indentation data and Pilkington plc for provision of coated samples.

APPENDIX: Soft Surface layer Modelling – Volume Law-of-Mixtures with No Constraints

A.1 Introduction

Following the work of Buckle [48] a number of simple models for the hardness of a coating on a substrate have been developed based on different law-of-mixtures models [54-57]. The most successful of these models are based on the volume law-of-mixtures where the extent of plastic deformation in the coating and substrate is determined by the proportions of the (assumed) hemispherical deforming volume below the indenter lying partly in the coating and partly in the substrate. In the simplest model the difference in properties between the coating and substrate are assumed not to significantly change the radius and shape of the deforming volume and simple geometry can be used to predict the hardness behaviour of the coating substrate composite [58]. This is the case when considering very thin soft layers on a harder substrate where the deforming volume in the substrate is significant and controls the plastic deformation in the thin surface layer.

A.2 Modelling of a thin soft layer on a harder substrate

Consider a hemispherical plastic zone, beneath the indenter, of radius, R_p . The deforming volumes in the coating and substrate, V_c and V_s , are given by the volumes of slices through a hemisphere as shown in Figure 11. Here, t is the coating thickness and H_c and H_s are the hardness of the coating and substrate respectively. The radius of the plastic zone is calculated from the maximum displacement, δ_{\max} , via [59]:

$$R_p = (4.5451 - 12.07H/E)\delta_{\max} \quad (\text{a.1})$$

Since the soft surface layer is very thin and behaviour is controlled by the underlying hard material we use H and E for the bulk, unsoftened material to determine the plastic zone radius. The plastic contact depth, δ_c (which is used to calculate hardness), is found to be a constant fraction of the maximum indenter displacement which include elastic and plastic contributions [36] and can be found from fits to experimental data.

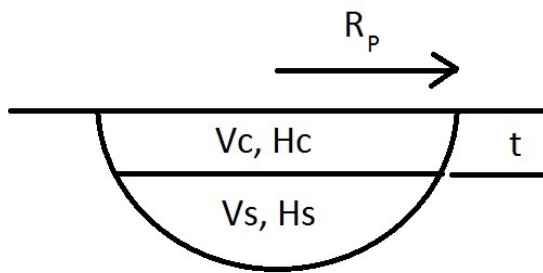


Figure 11: Deforming volumes and material properties for a single layer volume law-of-mixtures model.

For the situation in Figure 11 expressions for the deforming volumes can then be easily determined from the appropriate volume integrals.

$$V_c = \pi R^2 t - \pi t^3/3 \quad (a.2)$$

$$V_s = 2/3 \pi R^3 - \pi R^2 t + \pi t^3/3 \quad (a.3)$$

The total deforming volume, $V_t = V_c + V_s$ and thus for a hemispherical deforming volume

$$V_t = 2/3 \pi R^3 \quad (a.4)$$

Then the effective hardness of the coating/substrate composite, H_{eff} , is given by

$$H_{eff} = H_c V_c + H_s V_s / V_t \quad (a.5)$$

This may be extended to a double layer model where V_i , H_i and t_i are the deforming volume, hardness and thickness of a layer intermediate between the coating and substrate.

$$V_c = \pi R^2 t_c - \pi t_c^3/3 \quad (a.6)$$

$$V_i = \pi R^2 t_i - \pi t_c t_i + \pi t_i^3/3 - \pi t_i^3/3 \quad (a.7)$$

$$V_s = 2/3 \pi R^3 - \pi R^2 (t_c + t_i) + \pi (t_c + t_i)^3/3 \quad (a.8)$$

Thus

$$H_{eff} = H_c V_c + H_i V_i + H_s V_s / V_t \quad (a.9)$$

A.3 Application of the models

Most materials show a very thin adsorbate modified layer (AML) which is usually only a few nanometres thick. An example of this is the very thin water affected layer on fused silica seen in AFM scans of the fused silica nanoindentation standard in Figure 12. The origins of this layer are materials-sensitive and depend on adsorbed species on the surface, surface roughness and reconstructions, surface porosity and composition changes due to, for instance leaching or segregation. In the case of fused silica, the thin layer is around 2nm thick and can be scraped off by progressively increasing the force on the AFM cantilever during scanning. However, there is no apparent soft surface layer in the load displacement curves in fused silica. For the purpose of modelling it is assumed that the hardness of this layer is very low ($H_c = 0.5 \text{ GPa}$) and the hardness of the fused silica bulk is 10GPa. From experimental data for fused silica, $\delta_{max} = 1.3745 \delta_c$.

A single soft surface layer 2nm thick with hardness 0.5GPa on fused silica with hardness 10GPa is modelled in Figure 14 using equation (a5). The grey box marks the region where experimental data is usually observable including experimental errors based on a 10GPa hardness and 5% scatter in measurements. The vertical line marks the experimental boundary between elastic (LHS) and elastic-plastic (RHS) indentations – the precise position of the line is dependent of the tip end radius but, in Figure 13, a typical value for the minimum contact depth observed in elastic-plastic indentations in fused silica with a new Berkovich tip is used. Only valid experimental data is expected to the right of this line i.e. at higher contact depths.

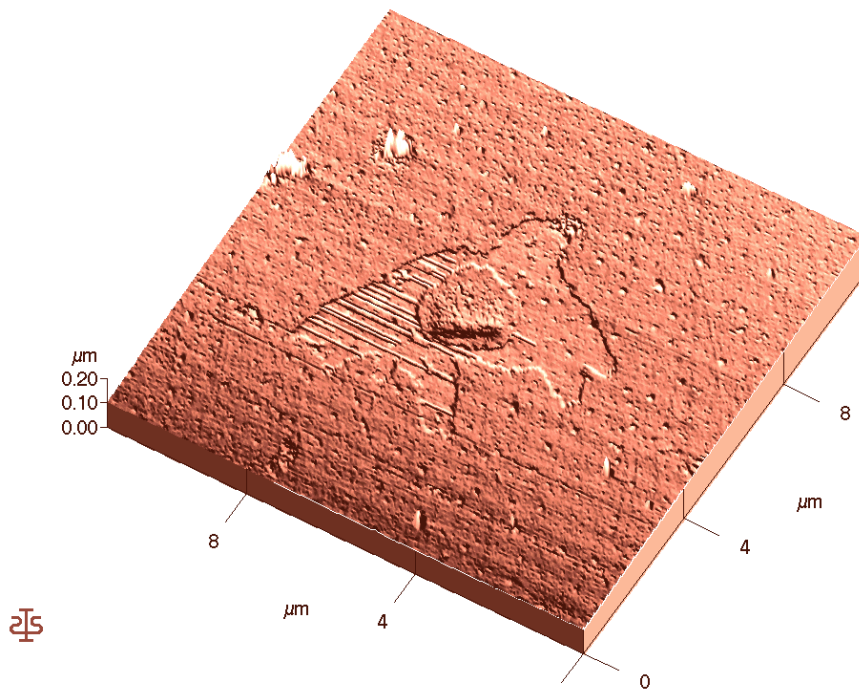


Figure 12: Contact mode AFM scan of the region around a spherical indentation in fused silica. A soft surface layer has been occasionally scratched off the surface of the substrate material during imaging. The intermittent nature of the layer removal probably arises from local differences in adhesion etc. Despite this observation, no soft layer was detected by low-load indentation.

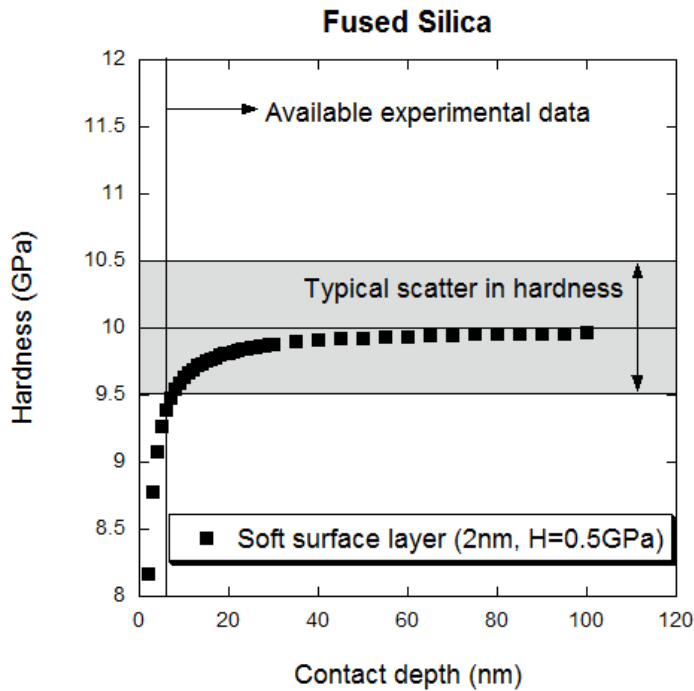


Figure 13: Predicted variation of hardness with contact depth for fused silica with a 2nm soft surface layer ($H_c=0.5\text{GPa}$, $H_s=10\text{GPa}$). The grey box marks the typical scatter in experimental data based on a 10GPa hardness with 5% variation. Only valid hardness measurements from plastic deforming indentations are observed to the right of the vertical line so the soft surface layer cannot be seen in the experimental data.

Elastic indentations are observed in low load tests and the smallest measurable contact depth for an elastic-plastic indentation for fused silica is around 5nm. Thus the modelled data to the left of the vertical line should be ignored as not measureable. To the right of the line the modelled data falls in the experimental scatter band for unsoftened material so no soft surface layer is likely to be observed.

In the same way, it is expected that the majority of adsorbate modified layers (AML) are likely to be invisible in the nanoindentation hardness data, even though they may have a significant effect on the tribological (friction) behaviour of the material.

There are cases where more significant surface softening is observed on a glassy material – for instance on float glass that has been dish-washed with deionised water (as part of the manufacturing process) for cleaning prior to coating deposition. This is shown in Figure 14, but the softening effect is usually small and only statistically significant when the contact depth is less than 20nm which is consistent with the results of modelling the effect of a slightly thicker ($\sim 5\text{nm}$) soft layer on a silica substrate. In this case there has been some leaching of the alkali modifier from the glass surface and reduction in surface density. Again, this would be statistically-undetectable in indentation experiments.

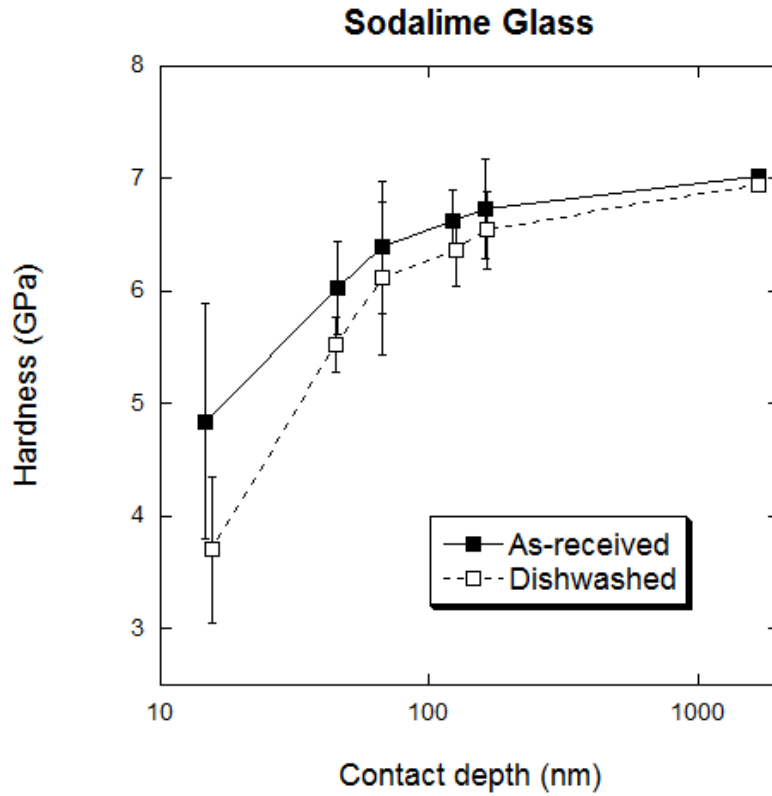


Figure 14: Effect of dishwashing on the surface hardness of soda-lime glass

For sapphire there is an approximately 5nm thick soft surface layer visible in the early part of the nanoindentation load-displacement curve. This cannot easily be explained by the adsorbate modified layer and it is suggested that a second mechanism is operating and this is evidence of a band-modified layer (BML) affecting dislocation mobility and hardness. This hypothesis can be tested by modelling two cases. In the single layer model (equation (a5)) a 1nm layer with 2GPa hardness is present on a bulk material with 25GPa hardness and 350GPa modulus. For the double layer model (equation (a9)) we insert a 5nm layer of 20GPa hardness between these. For sapphire, $\delta_{\max} = 1.242\delta_c$ from experimental data. These models are compared in Figure 15. Again the grey region marks the scatter in experimental data from an unsoftened substrate and the vertical line marks the boundary between elastic indentation (where hardness is not defined) and elastic-plastic indentation where valid hardness measurements are obtained.

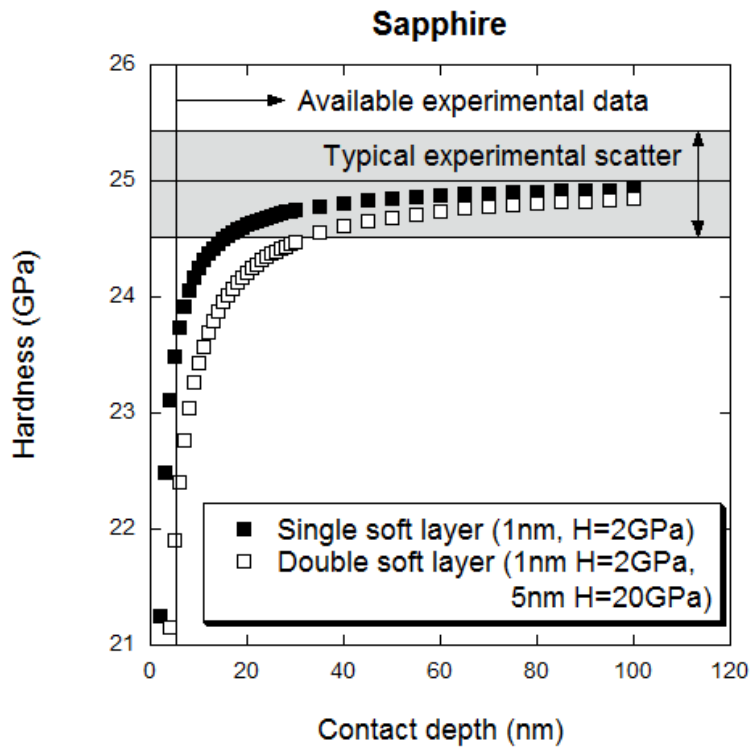


Figure 15: Variation of hardness with contact depth for sapphire with different soft surface layers.

In the single layer model the soft surface layer effect only persists to less than 15nm contact depth and would be only just measurable. The softening effect persists to 30nm contact depth exactly as observed in the hardness data in the double layer model. The effect of these layers should therefore be observable in the nanoindentation data as we have found.

The model could be updated to investigate the effect of a soft surface layer on the early stages of the load displacement curve to determine if this would be visible in experimental data. This is a topic for future work.

6. Conflicts of interest

The authors are aware of no conflicts of interest in respect of this work.

7. References.

- [1] Rehbinder P (1931) Verminderung der Ritzhärte bei Adsorption grenzflächenaktiver Stoffe. *Z Phys* 72:191-205.
- [2] Rehbinder P (1947) New physico-chemical phenomena in the deformation and mechanical treatment of solids. *Nature*, 159:866-867.
- [3] Fischer TE, Anderson MP, Jahanmir S, Salher R (1988) Friction and wear of tough and brittle zirconia in nitrogen, air, water, hexadecane and hexadecane containing stearic-acid. *Wear*, 124:133-148.
- [4] Sasaki S (1989) The effects of the surrounding atmosphere on the friction and wear of alumina, zirconia, silicon-carbide and silicon-nitride. *Wear*, 134:185-200.
- [5] Fischer TE (1988) Tribochemistry. *Ann Rev Mater Sci* 18:303-323.
- [6] Singer IL, Fayeulle S, Ehni PD (1991) Friction and wear behaviour of TiN in air - the chemistry of transfer films and debris formation. *Wear* 149:375-394.
- [7] Kim DS, Fischer TE, Gallois B (1991) The effects of oxygen and humidity on friction and wear of diamond-like carbon-films. *Surf Coat Technol* 49:537-542.
- [8] Westwood ARC, Macmillan NH, Kalyoncu RS (1973) Environment-sensitive hardness and machinability of Al_2O_3 . *J Am Ceram Soc* 56:258-262.
- [9] Macmillan NH, Huntington RD, Westwood ARC (1974) Chemomechanical control of sliding friction behavior in nonmetals. *J Mater Sci* 9:697-706.
- [10] Hanneman RE, Westbrook JH (1968) Effects of adsorption on the indentation deformation of non-metallic solids. *Phil Mag* 18:73-88.
- [11] Westbrook JH, Jorgensen PJ (1968) Effects of water desorption on indentation microhardness anisotropy in minerals. *Am. Mineralogist*, **53** 1899-1911.
- [12] Westwood ARC, Huntington RD, Macmillan NH (1973) Influence of environment on mobility of near-surface dislocations in ionic-crystals. *J App Phys* 44:5194-5195.
- [13] Westwood ARC, Ahearn JS, Mills JJ (1981) Developments in the theory and application of chemomechanical effects. *Colloids and Surfaces* 2:1-35.
- [14] Westwood ARC, Goldheim DL, Lye RG (1967) Rehbinder effects in MgO. *Phil Mag* 16:505-506.
- [15] Czernuska JT, Page TF (1984) A Problem in Assessing the Wear Behaviour of Ceramics: Load, Temperature and Environmental Sensitivity of Hardness. *Proc Br Ceram Soc* 34:145-56.
- [16] Czernuska JT, Page TF (1987) Characterizing the surface-contact behavior of ceramics 2: Chemo-mechanical effects. *J Mater Sci* 29:3917-3923.

- [17] Bowden FP, Tabor D (1954) *The Friction and Lubrication of Solids*. Clarendon Press, Oxford.
- [18] Hirth JP, Lothe J (1988) *Theory of Dislocations*. McGraw-Hill, New York.
- [19] Hirsch PB (1981) Plastic-deformation and electronic mechanisms in semiconductors and insulators. *J de Physique* 42:3149-3160.
- [20] Macmillan NH (1977) Chemisorption-induced variations in the plasticity and fracture of non-metals. In: Latanision RM, Fourie JT (eds) *Surface Effects in Crystal plasticity*. Leyden, Noordhof, pp 629-61.
- [21] Burnett PJ, Page TF (1985) Chemomechanical effect in ion-implanted magnesium oxide. *J Mater Sci Lett* 4:1364-1370.
- [22] Bull SJ, Page TF (1989) Chemomechanical effects in ion implanted MgO. *J Phys D Appl Phys* 22:941-947.
- [23] Hainsworth SV, Page TF (1994) Nanoindentation studies of the chemomechanical effect in sapphire. *J Mater Sci* 29:5529-5540.
- [24] Hainsworth SV, Page TF (1994) Nanoindentation studies of chemomechanical effects in thin-film coated systems. *Surf Coat Technol* 68:571-575.
- [25] Gerberich WW, Venkataraman SK, Huang H, Harvey SE, Kohlstedt DL (1995) The injection of plasticity by millinewton contacts. *Acta Metall Mater* 43:1569-1576.
- [26] Venkataraman SK, Kohlstedt DL, Gerberich WW (1993) Continuous microindentation of passivating surfaces. *J Mater Res* 8:685-688.
- [27] Mann AB, Pethica JA (1996) Nanoindentation studies in a liquid environment. *Langmuir* 12:4583-4586.
- [28] Mann AB (2004) Mechanics and geometry of nanoasperity contacts in organic fluids. *Appl Phys Lett* 85:5203-5205.
- [29] Mohanty B, Mann AB (2012) Chemomechanical effects of long-chain alcohols during nanoindentation. *J Mater Res* 27:222-228.
- [30] Page TF, Oliver WC, McHargue CJ (1992) The deformation-behavior of ceramic crystals subjected to very low load (nano) indentations. *J Mater Res* 7:450-473.
- [31] Williams JA (1994) *Engineering Tribology*, OUP, Oxford.
- [32] Tutein AB, Stuart SJ, Harrison JA (1999) Indentation Analysis of Linear-Chain Hydrocarbon Monolayers Anchored to Diamond. *J Phys Chem B* 103:11357-11365.
- [33] Liley M, Gourdon D, Stamou D, Meseth U, Fischer TM, Lautz C, Stahlberg H, Vogel H, Burnham NA, Duschl C (1998) Friction Anisotropy and Asymmetry of a Compliant Monolayer Induced by a Small Molecular Tilt. *Science* 280:273-275.

- [34] Belde KJ, Bull SJ (2006) Chemomechanical effects in optical coating systems. *Thin Solid Films* 515:859-865.
- [35] Page TF, Bull SJ (2006) Measuring and modelling the instrumented indentation (nanoindentation) response of coated systems. *Phil Mag* 86:5331-5346.
- [36] Oliver WC, Pharr GM (1992) An Improved Technique for Determining Hardness and Elastic Modulus Using Load and Displacement Sensing Indentation Experiments. *J Mater Res* 7:1564-1583.
- [37] Page TF, Riester L, Hainsworth SV (1998) The Plasticity Response of SiC and Related Isostructural Materials to Nanoindentation: Slip vs Densification. In: Baker SP, Burnham N, Gerberich WW, Moody N (eds) *Fundamentals of Nanoindentation & Nanotribology*. *Proc Mater Res Soc Symp* 522:113-118.
- [38] Jang J, Pharr GM (2008) Influence of indenter angle on cracking in Si and Ge during nanoindentation. *Acta Materialia* 56:4458-4469.
- [39] Sasaki S, Pethica JB (2000) Effects of surrounding atmosphere on micro-hardness and tribological properties of sintered alumina. *Wear* 241:204-208.
- [40] Johnson KL, Kendall, Roberts AD (1971) Surface energy and the contact of elastic solids. *Proc Roy Soc Lond A* 324:301-313.
- [41] Bull SJ, Page TF, Yoffe EH (1989) An explanation for the indentation size effect in ceramics. *Phil Mag Lett* 59:281-288.
- [42] Bull SJ (2003) On the origins and mechanisms of the indentation size effect. *Zeitschrift fur Metallkunde*, 94:787-792.
- [43] Sargent PM, Page TF (1985) Factors Affecting Hardness and Hardness Anisotropy. *J Mater Sci* 20:2388-2398.
- [44] Bull SJ (2015) Elastic properties of multilayer oxide coatings on float glass. *Vacuum* 114:150-157.
- [45] Bull SJ (2014) Size effects in the mechanical response of nanoscale multilayer coatings on glass. *Thin Solid Films* 571:290-295.
- [46] Czernuszka JT, Page TF (1985) The importance of microscopy in studying the wear behaviour of ceramics. *J Microsc* 140:159-169.
- [47] Rodgers KA (1993) Routine identification of aluminium hydroxide polymorphs with the laser Raman microprobe. *Clay Minerals* 28:85-99.
- [48] Buckle, H (1973) Use of the hardness test to determine other material properties. In: Westbrook, JH and Conrad H (eds) *The science of hardness testing and its research applications*. ASM, Ohio, p453-491.

- [49] Hutchings IM (1992) Tribology: Friction and wear of engineering materials, Edward Arnold, London, pp30-33.
- [50] Soare SM (2004) Design of a rotating sensor for stress measurement in metallisation. PhD thesis, Newcastle University.
- [51] Moharrami N, Langton D, Bull SJ, Sayginer O. (2013) Why does titanium alloy wear cobalt chrome alloy despite lower bulk hardness: a nanoindentation study? Thin Solid Films 549: 79-86.
- [52] Ramsey PM, Page TF (1992) The interaction between high speed nylon fibre and unlubricated ceramic textile guides. Textile Research Journal, 62:715-728.
- [53] Czernuszka JT, Page TF (1997) Wear of engineering ceramics by a soft abrasive. J Mater Sci 32:6671-6680.
- [54] Sargent PM (1979) Factors affecting the microhardness of solids, PhD Thesis, University of Cambridge.
- [55] Burnett PJ, Page TF (1984) Surface softening in silicon by ion-implantation. J Mater Sci 19:845-860.
- [56] Burnett PJ, Rickerby DS (1987) The mechanical-properties of wear-resistant coatings, Thin Solid Films, 148:41-50; 51-65.
- [57] Bull SJ, Rickerby DS (1990) New developments in the modelling of the hardness and scratch adhesion of thin films. Surf Coat Technol 42:149-164.
- [58] Bull, SJ (2001) Interface Engineering and Graded Films; Structure and Characterisation. J. Vac. Sci. Technol., A19: 1404-1414.
- [59] Chen J, Bull SJ (2006) On the relationship between plastic zone radius and residual depth during nanoindentation. Surf Coat Technol 201:4289-4293.